*Biological Journal of the Linnean Society*, 2020, **131**, 192–202. With 2 figures.

# Morphological characterization of flight feather shafts in four bird species with different flight styles

GERGELY OSVÁTH[1,2,3,*], ORSOLYA VINCZE[1,4], DRAGOMIR-COSMIN DAVID[5], LÁSZLÓ JÁCINT NAGY[1], ÁDÁM Z. LENDVAI[2,6], ROBERT L. NUDDS[7], and PÉTER L. PAP[1,2]

[1]*Evolutionary Ecology Group, Hungarian Department of Biology and Ecology, Babeş-Bolyai University, Clinicilor Street 5–7, RO–400006 Cluj-Napoca, Romania*
[2]*Department of Evolutionary Zoology and Human Biology, University of Debrecen, Egyetem Square 1, H–4032 Debrecen, Hungary*
[3]*Museum of Zoology, Babeş-Bolyai University, Clinicilor Street 5–7, RO–400006 Cluj-Napoca, Romania*
[4]*Department of Tisza Research, MTA Centre for Ecological Research-DRI, Bem Square 18/C, H-4026 Debrecen, Hungary*
[5]*Department of Taxonomy and Ecology, Faculty of Biology and Geology, Babeş-Bolyai University, Clinicilor Street 5–7, RO–400006 Cluj-Napoca, Romania*
[6]*Department of Geology, Babeş-Bolyai University, Mihail Kogalniceanu Street 1, 400084 Cluj-Napoca, Romania*
[7]*School of Biological Sciences, Faculty of Biology, Medicine & Health, University of Manchester, M13 9PL Manchester, UK*

*Received 12 February 2020; revised 11 June 2020; accepted for publication 16 June 2020*

Variation in rachis (central shaft) morphology in individual remiges (flight feathers) within and among species reflects adaptations to requirements imposed by aerodynamic forces, but the fine-scale variation of feather morphology across remiges is not well known. Here we describe how the shape of the rachis, expressed by the height/width ratio, changes along the longitudinal and lateral axis of the wing in four bird species with different flight styles: flapping-soaring (white storks), flapping-gliding (common buzzards), passerine-type (house sparrows) and continuous flapping (pygmy cormorants). Overall, in each wing feather, irrespective of species identity, rachis shape changed from circular to rectangular, from the base towards the feather tip. The ratio between the height and width of the calamus was similar across remiges in all species, whereas the ratio at the base, middle and tip of the rachis changed among flight feathers and species. In distal primaries of white storks and common buzzards, the ratio decreased along the feather shaft, indicating a depressed (wider than high) rachis cross section towards the feather tip, whereas the inner primaries and secondaries became compressed (higher than wide). In house sparrows, the rachis was compressed in each of the measurement points, except at the distal segment of the two outermost primary feathers. Finally, in pygmy cormorants, the width exceeds the height at each measurement point, except at the calamus. Our results may reflect the resistance of the rachis to in-plane and out-of-plane aerodynamic forces that vary across remiges and across study species. A link between rachis shape and resistance to bending from aerodynamic forces is further indicated by the change of the second moment of areas along the wing axes.

ADDITIONAL KEYWORDS: *Buteo buteo* – *Ciconia ciconia* – flight style – *Microcarbo pygmaeus* – *Passer domesticus* – rachis morphology – rachis shape – rachis width – second moment of area – wing feather.

## INTRODUCTION

To become airborne and move forward, birds need to generate lift and propulsive thrust to overcome their weight and drag forces, respectively (Pennycuick, 2015). Flight feathers provide the largest part of the lifting surface of bird wings, which have to withstand aerodynamic forces during flight (Lindhe Norberg, 2002; Wang *et al.*, 2012; Altshuler *et al.*, 2015). The distribution of forces acting upon the wing changes

*Corresponding author. E-mail: osvathgergely@gmail.com

 

across the wing, and the pattern of this change is influenced by flight style, i.e. whether a bird flies with continuous wing flapping, or soars/glides without flapping its wings. Thus, it can be hypothesized that the structural parameters of the feather shaft varies with the flight style of birds (Ennos *et al.*, 1995; Pap *et al.*, 2015).

Resistance to bending and torsion under cyclic aerodynamic loads is provided by the rachis, the central shaft of a feather. Overall diameter and the cross-sectional shape are the main determinants of the bending pattern of the rachis (Corning & Biewener, 1998; Tubaro, 2003; De la Hera *et al.*, 2010; Sullivan *et al.*, 2017; Wang & Meyers, 2017a). Furthermore, the differential flexural stiffness in the two planes of bending (i.e. dorso-ventral and lateral) is achieved mainly by changes in the cross-sectional morphology of the rachis (Purslow & Vincent, 1978). Therefore, variation in rachis shape between species and among flight feathers that are differently positioned along the wing should reflect adaptations to the requirements imposed by localized differential aerodynamic forces. Consequently, we predict that rachis morphology varies: (1) along the longitudinal axis of individual flight feathers; (2) among flight feathers across the wing span, and (3) between species characterized with different flight styles.

According to Bruderer *et al.* (2010), four main flight styles can be distinguished in birds: flapping and soaring, flapping and gliding, continuous flapping, and passerine-type flight. Flapping-soaring flight is used by relatively large species (e.g. vultures, storks) and is energetically the most efficient flight style, characterized by reduced flapping frequency. Flapping-gliding flight involves relatively long flapping periods and comparably long gliding phases with outstretched wings (e.g. gulls and falcons). Smaller passerine birds have a specific flight style which is characterized by short flapping phases followed by a short parabolic flight path with closed wings and gliding with outstretched wings. Continuous flapping birds flap their wings with constant wing-beat frequency over relatively long distances (e.g. waders, ducks and cormorants). Each of these flight styles is associated with different aerodynamic and inertial properties, which in turn influence the structural properties of the rachis (Pap *et al.*, 2015; Pennycuick, 2015; Lees *et al.*, 2016).

A comprehensive comparative study using 137 species reported that the dorso-ventral rachis diameter (reflecting the bending resistance in dorso-ventral plane) of the innermost primary feathers is greater in soaring and gliding species than in species of continuous flappers and passerine-type flyers (Pap *et al.*, 2015). Furthermore, the study of Pap *et al.* (2015) found a marked increase in rachis width from inner to outer primary feathers in flapping flyers, while in soarers and gliders the change along the wing is less pronounced. The latter result suggests that the aerodynamic forces are distributed more evenly across the primary feathers of soarers and gliders, whereas loading is more biased towards the distal primaries in flapping flyers. However, it remains undocumented how rachis shape varies across the entire wing. This variation might reflect differential adaptation of flight feathers to in-plane (load acting perpendicular to the wing plane) and out-of-plane aerodynamic forces (loads that are applied parallel to the wing plane), see Fig. 1 (Purslow & Vincent, 1978; Ennos *et al.*, 1995).

Distal (primary) and proximal (secondary) feathers have distinct functions in flight, and so have to withstand forces acting from different directions (Norberg, 1985; Videler, 2005; Usherwood, 2010; Muijres *et al.*, 2012). Primary feathers are responsible for generating not only thrust but also lift (Norberg, 1985; Videler, 2005), whereas proximal wing feathers (secondaries) mostly generate lift (Müller & Patone, 1998). These differences correlate with the structural variation in the vanes between these two wing feather groups (Ennos *et al.*, 1995; Bachmann *et al.*, 2007; Heers & Dial, 2011; Feo *et al.*, 2015), but little is known about the variation of their rachis shape.

The aerodynamic load also varies along the axis of individual feathers (Müller & Patone, 1998; Sullivan *et al.*, 2017), which is reflected in the change in the structural and mechanical properties along the rachis (Purslow & Vincent, 1978; Macleod, 1980; Bonser & Purslow, 1995; Cameron *et al.*, 2003; Bachmann *et al.*, 2012). The bending stiffness of the rachis primarily depends on how the material is distributed in the cross-section (i.e. second moment of area) and changing the cross-sectional shape is an effective solution for adjusting the bending stiffness of a rachis to accommodate differential aerodynamic forces (Purslow & Vincent, 1978; Bonser & Purslow, 1995; Weber *et al.*, 2010). It was shown that the shape of the flight feather rachis changes from round to square/rectangular from feather base to feather tip (Wang & Meyers, 2017b). This rectangular form offers greater bending stiffness per unit area and allows flight feathers to twist and resist flexure (Wang *et al.*, 2016; Sullivan *et al.*, 2017; Wang & Meyers, 2017a, b). To date, however, morphological investigations have principally focused on primary feathers, or often on a single feather of the wing. It is still unclear how the shape varies along the rachis within individual feathers, among all of the feathers across the wing, and how these traits differ among species.

Here, we investigated the variation of the rachis shape (1) along the longitudinal axis of individual flight feathers, (2) across remiges and (3) among four bird species with remarkably different flight styles:

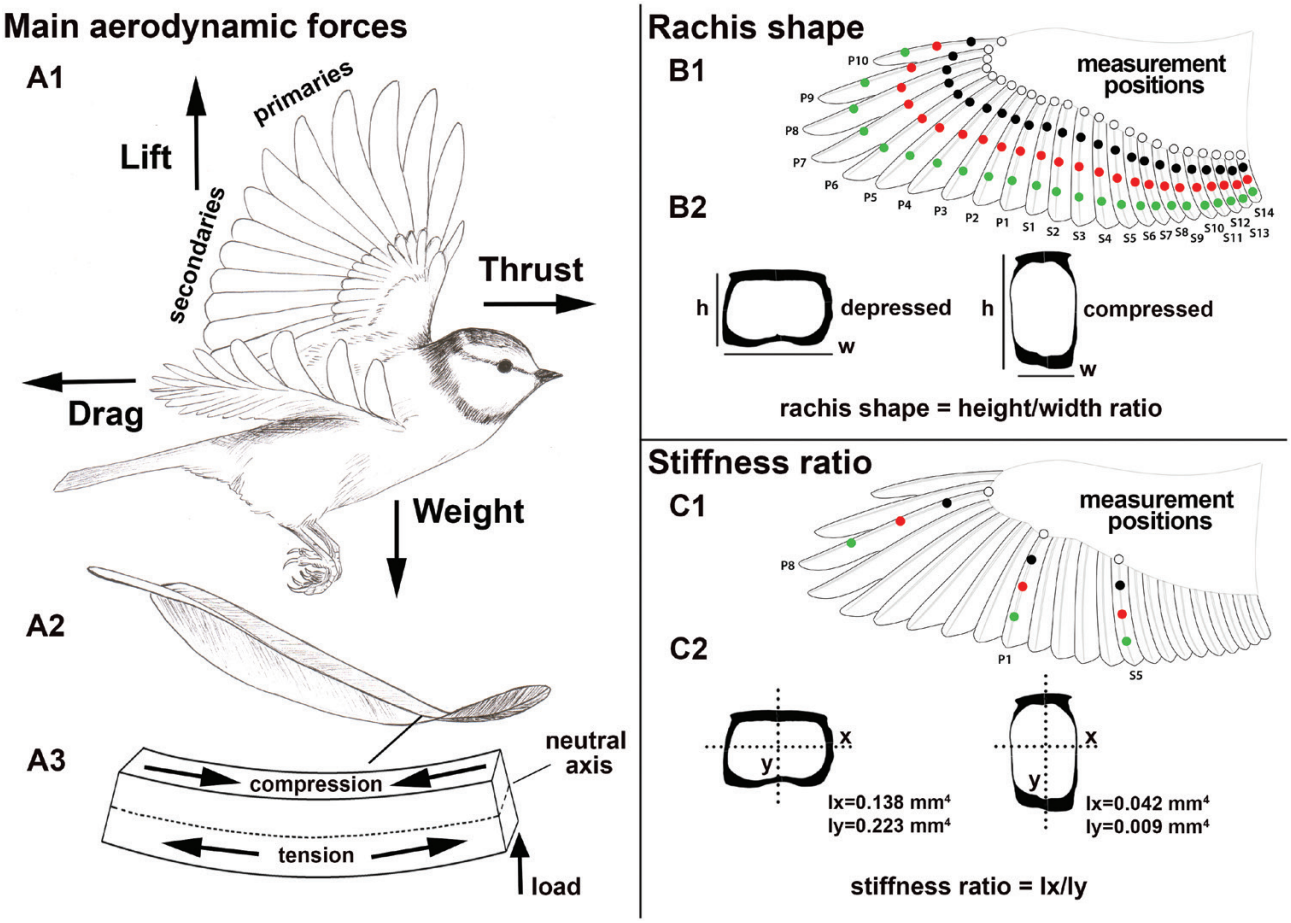


**Figure 1.** A1, main aerodynamic forces acting on wing feathers. A2, the bending of a feather under aerodynamic load. A3, schematic lateral view of a bent rachis segment. B1, the dots show the measurement positions of rachis shape along the wing (open—calamus, black—base, red—middle, green—tip). B2, the method for calculating rachis shape. C1, positions along the wing from where rachis cross-sections were taken to measure the second moment of area. C2, cross-section of common buzzard rachises at the tip of P1 (right) and P8 (left) after image processing. x is the neutral axis for bending in dorsoventral direction (span-wise bending), y is the neutral axis for bending in lateral direction (chord-wise bending). Ix is the second moment area with respect of x axis (stiffness in dorso-ventral direction), Ix is the second moment area with respect of y axis (stiffness in lateral direction).

flapping-soaring [white stork (*Ciconia ciconia*)], flapping-gliding [common buzzard (*Buteo buteo*)], passerine-type [house sparrow (*Passer domesticus*)] and continuous flapping [pygmy cormorant (*Microcarbo pygmaeus*)]. In order to describe the variation in rachis' shape, we calculated the dorso-ventral/lateral width ratio (i.e. height/width ratio) at four measurement positions (calamus, base, middle and tip defined as the 0%, 25%, 50% and 75% points of the total vane length, respectively) along the rachis, where a value higher than one indicates higher than wider rachis section ('compressed' shape), and values smaller than one indicate wider than higher rachis section ('depressed' shape) (Fig. 1).

We expect that the greatest cross-sectional diameters of remiges are in those planes where the bending forces are largest. Since, in general, inner primaries and secondaries cope with stronger lift forces, we predict that the rachis of secondaries tends to be higher than wide (i.e. compressed shape) in each examined species and at each measurement position of these feathers. Because the outermost primary constitutes the leading edge of the wing, these are likely to experience significant lateral aerodynamic forces from drag, we expect a smaller height to width ratio (i.e. more depressed shape) of the rachis of outermost primary than in primaries proximal to it, which in turn should have a more compressed shape, similar to inner primaries and secondaries. However, we predict in soaring and gliding white storks and common buzzards, a depressed rachis shape in all distal primaries which constitutes the slotted

wingtip (the six, respectively five distal primaries in white storks and common buzzards). The rationale behind this expectation is that in a slotted wingtip each feather acts as an individual aerofoil, being exposed to large lateral forces, while moving through the air. In the flapping and passerine-type flyer house sparrows and pygmy cormorants, we predict a compressed shape in all primaries other than the outermost, since the more active flapping flight is associated with stronger bending and twisting forces.

## MATERIAL AND METHODS

### Data collection and feather measurements

We collected wing feathers from carcasses of white storks ($N$ = 11), common buzzards ($N$ = 10), house sparrows ($N$ = 10) and pygmy cormorants ($N$ = 10). Only individuals with fully grown remiges were considered. We plucked all remiges (primaries and secondaries) from one of the two wings from each individual bird, totalling 33 feathers from white storks (11 primaries and 22 secondaries), 24 from common buzzards (10 and 14), 25 from pygmy cormorants (10 and 15) and 18 from house sparrows (9 and 9). The innermost secondary (S22) in white storks was missing in eight birds, while the outermost primary (P10) in the house sparrows is vestigial, therefore these feathers were excluded from the analysis. White storks were either juveniles, sub-adults or adults; common buzzards and pygmy cormorants were juveniles or adults, while all house sparrows were in adult plumage.

For each feather collected, we measured the dorso-ventral (= height) and lateral width (= width) of the rachis with a digital caliper (to the nearest 0.01 mm) at four positions along the rachis. Then we calculated the height/width ratio as a proxy of rachis shape, by dividing these two values for each measurement point. These positions are at the base of the vane (calamus), and along the rachis at one-quarter (base), half (middle) and three-quarters of the distance from the base to the tip (Fig. 1). The rachis widths of white storks' feathers were measured by Dragomir-Cosmin David, the common buzzards and house sparrows were measured by Gergely Osváth, and the pygmy cormorants by László Jácint Nagy. Repeatability between observers (i.e. measurements of the same feathers by different observers) was high for all parameters [rachis height: Intra-class Correlation Coefficients (ICC) = 0.99; 95% CI 0.988–0.999; rachis width: ICC = 0.99; 95% CI 0.991–0.999]. Measurements generally showed very high intraspecific repeatability (ICC > 0.78) in all tested feathers and positions. All data are reported in the Supporting Information (Table S1).

### Determination of the second moment of area

To illustrate the variation in cross-sectional shape of the rachis, we used the third outermost primary (P7, P8 or P9 depending on species; see Fig. 1 and Fig. 2), the innermost primary (P1), and the fifth secondary feather (S5) from one individual of each species. Feathers were prepared by removing the vanes and by creating cross sections at four positions along the vane; at the calamus, base, middle and tip. Feather pieces were embedded in epoxy and cross-sections were polished using graded sand papers, then each cross-section was photographed. These images were also used to calculate the second moment of area of the different rachis segments in order to confirm the pattern of variation in the dorso-ventral and lateral bending resistance suggested by dorso-ventral/lateral rachis width ratio (i.e. height/width ratio) (Fig. 1). The second moment of area (I, $mm^4$) is an important parameter in structural engineering, which quantifies the bending resistance of a beam about a given axis of a cross-section: assuming homogeneous material properties, structures with larger values of I are stiffer than those with smaller values of I (Young, 1989). The feather shaft is structurally a tapered cantilever beam in which case the magnitude of I is a reflection of the amount of material (keratin) in cross-section and its distribution perpendicular to a given neutral axis (the square area of keratin resisting compression or tension in the plane of bending) (Pennycuick, 2008). In our study Ix and Iy are measures of the second moment of area about the x and y axis (Fig. 1). Therefore, Ix indicates the stiffness in a dorso-ventral plane, whereas Iy reflects the stiffness of a given cross-section in lateral flexion. The second moment area values were calculated using BoneJ, a plugin of Fiji-ImageJ (Doube *et al.*, 2010; Schindelin *et al.*, 2012). We calculated the stiffness ratio (Ix/Iy), and a value greater than one indicates greater dorso-ventral bending stiffness, whereas values smaller than one indicate greater lateral bending stiffness (Blanco *et al.*, 2009).

### Statistical analysis

The morphology of feathers can vary depending on the age of a bird (Butler *et al.*, 2008) and because our dataset includes white storks, common buzzards and pygmy cormorants with both juvenile and adult wing feathers, we tested for differences between different age classes. Rachis shape was similar in adult and juveniles birds (paired $t$-test): common buzzards: t = -0.23, df = 95, $P$ = 0.81; pygmy cormorants: t = -0.97, df = 91, $P$-value = 0.33; white storks: t = -1.2811, df = 127, $P$-value = 0.20). Therefore, it is unlikely that our results are affected by age-specific changes in feather traits.

Non-linear relationships were found between the dependent variable and the explanatory variables.

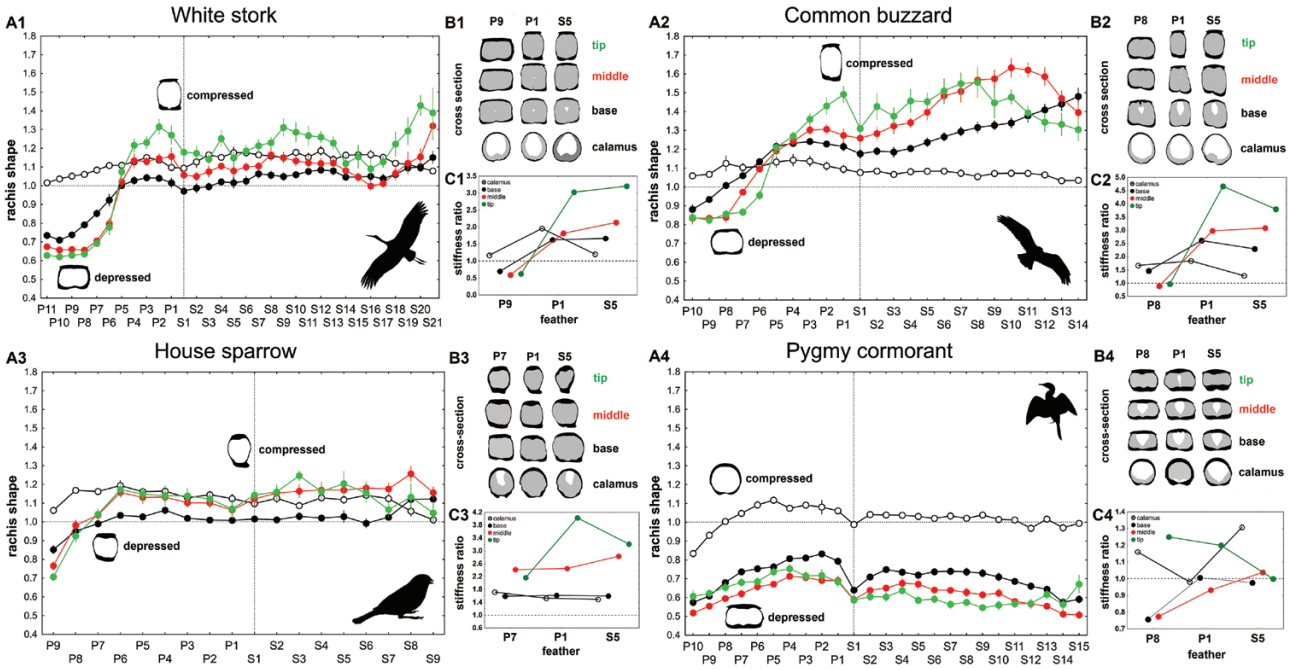


**Figure 2.** A1-A4, variation in rachis shape of wing feathers of the four examined species in relation to position along the rachis and position along the wing (P = primary; S = secondary). The symbols and colours indicate different position along the feather axis (open—calamus, black—base, red—middle, green—tip, as in Fig. 1). The vertical hatched line marks the border between the primary and secondary feathers. Mean ± SE are presented ($N$ = 11 for A1 and $N$ = 10 for A2-A4). B1-B4, cross-section of the rachis of the third outermost and the innermost primary along with the medial secondary feather. C1-C4, variation in Ix/Iy ratio among the second to outermost, the innermost primary and the medial secondary feather wing feathers. A higher value than 1 indicates greater dorso-ventral bending resistance, while values smaller than 1 indicate greater lateral bending resistance. Bird silhouettes taken from PhyloPic (http://phylopic.org)

Therefore, to investigate the variation of rachis shape across remiges, among the four measurement positions along the vane and among the four bird species, we performed General Additive Models (GAMs). Rachis shape values were used as dependent variables in the model that included species, feather identity (the individual number of each flight feather), measurement position (calamus, base, middle, tip) and the interaction between explanatory variables: rachis shape ~ species + measurement position + s(feather id) + s(feather id, measurement position) + s(feather id, species). GAMs were carried out using the 'gam' function with a Gaussian error distribution and smoothing function with default settings from the R package 'mgcv' (Wood, 2003, 2004, 2011, 2017; Wood *et al.*, 2016). All statistical analyses were conducted using the R statistical computing environment, v.3.4.2 (R Development Core Team, 2017).

## RESULTS

### Variation in rachis shape along the vane, among flight feathers and species

In the four study species, for each examined wing feather, the rachis shape changed from circular/oval to square/rectangular in shape, from the calamus towards the feather tip (Fig. 2). The height/width ratio of the rachis differed significantly among the four feather segments and wing feathers in each species (Table 1). Furthermore, the variation of rachis shape along the longitudinal axis of the rachis and across remiges showed different patterns among species (Fig. 2). All species showed a slightly compressed rachis at the calamus except pygmy cormorants (P10, P9 and S1). In the distal primaries of white storks and common buzzards, the height/width ratio decreased along the feather shaft, indicating that the rachis shape was becoming depressed towards the feather tip, while the inner primaries and secondaries became compressed (Fig. 2A1-A2). In house sparrows, the variation of the height/width ratio among flight feathers was similar, and the rachis was generally compressed at each of the measurement points, except at the distal segments of the two outermost primary feathers (Fig. 2A3). For all species the outermost primaries generally were depressed towards the feather tip (Fig. 2). In pygmy cormorants the height/width ratio at the calamus was close to one (except in the distal primaries) resulting in an almost circular profile, while towards the tip, the feathers showed more accentuated

**Table 1.** Results of the general additive models explaining the variation in rachis shape as a function of feather identity (i.e. the individual number of each flight feather), measurement position (i.e. position along the shaft: calamus, base, middle, tip) and species. Estimated degrees of freedom (edf); reference degrees of freedom (Ref.df)

| Terms | Rachis shape | | | |
|---|---|---|---|---|
| A. Parametric coefficients | Estimate | SE | *t*-value | *P*-value |
| Intercept | 0.19 | 0.0011 | 163.87 | <0.0001 |
| Measurement position | 0.22 | 0.0015 | 146.94 | <0.0001 |
| Species | 0.12 | 0.0015 | 82.19 | <0.0001 |
| B. Smooth terms: | edf | Ref.df | *F*-value | *P*-value |
| Feather id | 4.99 | 6.09 | 2.68 | 0.0129 |
| Feather id: measurement position | 24.63 | 25.84 | 104.07 | <0.0001 |
| Feather id: species | 25.16 | 26.15 | 163.85 | <0.0001 |

lateral rachis width associated with a depressed rachis shape. The height/width ratio of these segments varied between 0.5 and 0.8, indicating a width twice as large as the height in some feathers of pygmy cormorants (Fig. 2A4). For the other three species, the flattening of the feathers distally in the dorso-ventral plane is much less extreme than that of cormorants.

### Variation in stiffness ratio of the rachis

In white storks and common buzzards, the value of stiffness ratio (Ix/Iy) was below one at the distal part of the third outermost primary, but greater than one at each measurement point of the innermost primary and medial secondary feather (Table 2; Fig. 2C1-C2). This indicates greater bending stiffness in the lateral direction at the distal part of the outer primary, but relatively greater bending resistance in the dorso-ventral direction in the inner primary and secondary feathers. In house sparrows, the stiffness ratio values indicate greater bending stiffness in the dorso-ventral direction for each feather, and at each measurement point (Table 2; Fig. 2C3). In pygmy cormorants, the stiffness ratio was less than one at the base and middle of the third outermost primary, at the calamus and middle segment of the innermost primary and the base of S5, indicating greater bending resistance in the lateral direction. In contrast, the stiffness ratio indicates superior bending resistance in the dorso-ventral direction at the calamus of the third outermost, tip of the innermost and middle and base of S5. The base and middle segment of P1 and the tip of S5 show similar bending resistance in both directions (Table 2; Fig. 2C4).

## DISCUSSION

### Change in rachis shape along feather axis

We found that the cross-sectional shape of the rachis differs not only along the feather length, but also between wing feathers and species. In general, at the calamus, the rachis was oval in shape or circular in all four species, resulting in similar height and width. A compressed rachis shape was expected in all investigated birds, because of the large dorso-ventral forces acting on the feathers during downstroke, which are redirected towards the bones and tendons of the wing through the calamus (Bachmann *et al.*, 2012; Sullivan *et al.*, 2017). The relatively uniform cross-sectional shape of the calamus across the wing and among species suggests that the force exerted at the base of each feather is of similar orientation relative to the cross-sectional axes irrespective of feather size and position along the wing. The similar orientation of forces selects for the one optimum cross-section (i.e. the shape of the calamus is optimized to resist bending loads in a dorso-ventral direction). This is a realistic assumption, because flight feathers function like tapered cantilevered beams (Lees *et al.*, 2017), so the total force on the feather will be focused at the calamus (the point at which the feather leaves the skin) and the feathers are fixed against rotation at this point (Raikow, 1985). In contrast, the observed variation across the flight feathers and along the rachis suggests that the distribution and orientation of the aerodynamic forces relative to the cross-sectional axes differs both between feathers within a species as well as between species. Again, this is a reasonable assumption, because feather rachises are curved, meaning that forces applied to them, particularly distally, will twist as well as bend the feather (Corning & Biewener, 1998). The degree of twisting and bending depends on feather position with the distal primaries of many species splitting and parting to create wing-tip slots and the amount of this feather deflection differs between species (Withers, 1981; Norberg, 1985; Tucker, 1993, 1995; Lindhe Norberg, 2002). Flattened rachises ensuring resistance to torsional forces during twisting at the distal position of outer primaries found in the species studied here supports this notion.

**Table 2.** Measurements of the second moment of area in three feathers of each of the four studied species. See *Material and Methods* for sources

| Species | Measurement position | Third to outermost primary | | | Innermost primary | | | Medial secondary | | |
|---|---|---|---|---|---|---|---|---|---|---|
| | | $I_x$ ($mm^4$) | $I_y$ ($mm^4$) | $I_x/I_y$ ratio | $I_x$ ($mm^4$) | $I_y$ ($mm^4$) | $I_x/I_y$ ratio | $I_x$ ($mm^4$) | $I_y$ ($mm^4$) | $I_x/I_y$ ratio |
| White stork | Calamus | 26.0470 | 22.3000 | 1.1700 | 21.6780 | 11.0440 | 1.9600 | 7.0540 | 5.8990 | 1.2000 |
| | Base | 7.0140 | 10.0670 | 0.7000 | 6.1820 | 3.8090 | 1.6200 | 2.7850 | 1.6650 | 1.6700 |
| | Middle | 1.2350 | 2.1060 | 0.5900 | 2.3200 | 1.2770 | 1.8200 | 0.8870 | 0.4140 | 2.1400 |
| | Tip | 0.1380 | 0.2230 | 0.6200 | 0.2270 | 0.0750 | 3.0300 | 0.1090 | 0.0340 | 3.2100 |
| Common buzzard | Calamus | 5.7880 | 3.4650 | 1.6704 | 2.5860 | 1.4020 | 1.8445 | 1.7770 | 1.3950 | 1.2738 |
| | Base | 1.6190 | 1.1100 | 1.4586 | 1.3960 | 0.5350 | 2.6093 | 0.8120 | 0.3530 | 2.3003 |
| | Middle | 0.3530 | 0.3950 | 0.8937 | 0.3690 | 0.1240 | 2.9758 | 0.1910 | 0.0620 | 3.0806 |
| | Tip | 0.0290 | 0.0300 | 0.9667 | 0.0420 | 0.0090 | 4.6667 | 0.0190 | 0.0050 | 3.8000 |
| House sparrow | Calamus | 0.0426 | 0.0248 | 1.7187 | 0.0157 | 0.0103 | 1.5302 | 0.0104 | 0.0070 | 1.4892 |
| | Base | 0.0099 | 0.0062 | 1.5896 | 0.0061 | 0.0038 | 1.6148 | 0.0068 | 0.0042 | 1.5933 |
| | Middle | 0.0025 | 0.0010 | 2.4135 | 0.0015 | 0.0006 | 2.4495 | 0.0015 | 0.0005 | 2.8287 |
| | Tip | 0.0004 | 0.0002 | 2.1625 | 0.0004 | 0.0001 | 4.0283 | 0.0003 | 0.0001 | 3.2171 |
| Pygmy cormorant | Calamus | 0.5200 | 0.4480 | 1.1607 | 0.5470 | 0.5580 | 0.9803 | 0.2550 | 0.1950 | 1.3077 |
| | Base | 0.1060 | 0.1400 | 0.7571 | 0.1770 | 0.1760 | 1.0057 | 0.0800 | 0.0820 | 0.9756 |
| | Middle | 0.0410 | 0.0530 | 0.7736 | 0.0550 | 0.0590 | 0.9322 | 0.0270 | 0.0260 | 1.0385 |
| | Tip | 0.0050 | 0.0040 | 1.2500 | 0.0060 | 0.0050 | 1.2000 | 0.0030 | 0.0030 | 1.0000 |

### Patterns of rachis shape variation across remiges and between study species

The height to width ratio of the outer primaries of white storks, common buzzards and house sparrows decreased (i.e. depressed shape) towards the feather tip, whereas the height generally exceeded the width (i.e. compressed shape) in the inner primaries and the secondaries. Furthermore, in white storks and common buzzards, not only the rachis of the outermost primary, but also the rachises of all emarginated distal primaries were wider than they were high. Additionally, the ratio of second moments of area showed greater resistance to lateral forces (i.e. force that acts in the direction parallel to wing) in the outermost primary (third to outermost) and superior resistance to dorso-ventral bending in the innermost primary (P1) and medial secondary (S5). Hence, the rachis of the outer primaries appears to be relatively more resistant to lateral forces, while the rest of the wing feathers (i.e. inner primaries and secondaries) are stiffer in dorso-ventral than in lateral flexion. A generally compressed shape, indicative of greater bending resistance dorso-ventrally in wing flight feathers, is expected because the resultant relative forces on the wing are oriented dorso-ventrally, particularly during the wing's downstroke (Norberg, 1985). However, as aforementioned, the distal primaries split and spread (Withers, 1981) and they are oriented perpendicular to the direction of travel, so it is likely they experience significant lateral aerodynamic forces from drag even when not spread (Purslow & Vincent, 1978). Rachis morphology is also likely influenced by the need to resist torsional forces during twisting and because torsion reduces the bending moment required to cause buckling failure (Young, 1989), perhaps to increase resistance to lateral buckling. It should be noted, however, that although feather diameters and second moment of area (at the umbilicus) provide a broad indication of a flight feather's material properties within a species, across species comparisons are limited, because microstructure (keratin fibre matrix) likely differs markedly between species (Lees *et al.*, 2017). Therefore, a broader rachis in one direction or greater second moment of area does not necessarily mean increased stiffness or strength when comparing across species.

Among the outer primaries, the height/width ratio gradually increased from the outermost towards the inner primaries, and from the tip to the base of individual feathers. Hence, the cross section of the distal segment of the rachis progressively changes from depressed to compressed from the outermost towards the inner primary feathers. This pattern of variation was most pronounced among the emarginated remiges that form the wingtip in white storks and common buzzards. When separated to create wing-tip slots, each primary feather acts like an individual aerofoil (Tucker, 1995). Pennycuick (2008) suggested that the flexibility of feather shafts in outer primaries is graduated, which allows them to form the slotted wingtip passively by variations in the bending resistance of the shafts: the first feather bends until its tip points almost straight upwards, and subsequent feathers bend less, resulting in a cascade of up to six feathers around the wing tip. Hence, a depressed rachis shape may equate to an increase in flexibility, which makes our rachis cross-section analyses congruent with Pennycuick's (2008) hypothesis. A depressed rachis shape of distal primaries may also result in decreased profile drag allowing more efficient flight in laminar air flow (Bonser & Purslow, 1995; Cameron *et al.*, 2003).

In pygmy cormorants, width exceeds the height at each measurement point except at the calamus, representing a surprising pattern of a species characterized by high wing-beat frequencies, and therefore high aerodynamic loading on the wing's feathers from the dorso-ventral direction (Usher wood, 2003; Pap *et al.*, 2015, 2019). Pygmy cormorants dive and swim underwater using foot-propulsion, while the wings are held close to the body (Kato *et al.*, 2006). Therefore, swimming is unlikely to significantly influence flight feather morphology in terms of hydrodynamic forces, particularly as aerodynamic forces during flight will be far greater than forces experienced when submerged. It is possible that morphological adaptations of feather vanes to aquatic life [e.g. increased barb and barbule density (Pap *et al.*, 2015, 2017)], that aid water repellence or reduce buoyancy (i.e. reduce the amount of air trapped) during diving, also influence rachis morphology; however, further work is needed before this can be unequivocally concluded.

## CONCLUSION

We found that the cross-sectional shape of the rachis varies along the longitudinal axis of the feathers and along the wing of the four species studied. The morphology of the rachis appears to be driven by the orientation of *in situ* aerodynamic forces and the need to provide sufficient rigidity to resist them. The calamus was oval and slightly compressed in all birds and all remiges, indicating a shape optimized to resist bending loads in a dorsoventral direction. In white storks, common buzzards and house sparrows the

distal part of the outermost primaries, which forms the leading edge of the wing, had a depressed rachis shape and were relatively more resistant to lateral forces, while the rachis of the rest of wing feathers was compressed and stiffer in dorso-ventral than in lateral flexion. In addition, the gradual increase in the height to width ratio among the emarginated primaries of white storks and common buzzards suggest adaptation to bending that allows the slotted wingtip to be formed passively. Contrary to our predictions, in pygmy cormorants we found a depressed rachis shape at each measurement position, except at the calamus, which is perhaps an adaptation to aquatic locomotion. However, further research is needed in order to corroborate this hypothesis.

In conclusion this study adds new details to our understanding of the functional morphology of the rachis of flight feathers and overall, highlights the striking variation in feather structural morphology within individual feathers; across the wing and between examined species of birds. Hopefully, our study will be a catalyst for future work investigating the driving forces behind this diverse structural morphology, which will ultimately contribute to our understanding of avian wings and aerodynamics.

## ACKNOWLEDGEMENTS

We thank the members of the 'Milvus Group' Bird and Nature Protection Association, Tibor Fuisz, János Déri, Gábor Bakacsi, Andrea Józsa, Ildikó Mező and Márta Osváth-Ferencz for their considerable help in data collection. We also wish to thank Csongor I. Vágási, who read an early version of the manuscript and gave us numerous valuable suggestions. We are thankful to Erzsébet Ferencz, Kinga Kelemen and Valentin Kiss for the bird and wing drawings. The constructive comments raised by the Editor and two anonymous reviewers considerably improved the manuscript. G.O. was supported by the Collegium Talentum 2018 Programme of Hungary, and by the Pál Juhász-Nagy Doctoral School of Biology and Environmental Sciences of the University of Debrecen, Hungary. O.V. and P.L.P. were supported by the János Bolyai Research Scholarship of the Hungarian Academy of Sciences. O.V. was supported by the New National Excellence Programme of the Hungarian Ministry of Innovation and Technology (ÚNKP-19-4-DE-538). This research was funded by the Romanian Ministry of Research and Innovation (PN-III-P4-ID-PCE-2016-0404). Á.Z.L. was supported by the Hungarian Scientific Fund Grant (OTKA K113108), the Romanian Ministry of Education (PN-III-P4-ID-PCE-2016-0572) and the European Union and the European Social Fund (EFOP-3.6.1-16-2016-00022). The authors declare that they have no competing interests.

## REFERENCES

**Altshuler DL**, **Bahlman JW**, **Dakin R**, **Gaede AH**, **Goller B**, **Lentink D**, **Segre PS**, **Skandalis DA. 2015.** The biophysics of bird flight: functional relationships integrate aerodynamics, morphology, kinematics, muscles, and sensors. *Canadian Journal of Zoology* **93:** 961–975.

**Bachmann T**, **Klän S**, **Baumgartner W**, **Klaas M**, **Schröder W**, **Wagner H. 2007.** Morphometric characterisation of wing feathers of the barn owl *Tyto alba pratincola* and the pigeon *Columba livia*. *Frontiers in Zoology* **4:** 23.

**Bachmann T**, **Emmerlich J**, **Baumgartner W**, **Schneider JM**, **Wagner H. 2012.** Flexural stiffness of feather shafts: geometry rules over material properties. *The Journal of Experimental Biology* **215:** 405–415.

**Blanco RE**, **Jones WW**, **Rinderknecht A. 2009.** The sweet spot of a biological hammer: the centre of percussion of glyptodont (Mammalia: Xenarthra) tail clubs. *Proceedings of the Royal Society B: Biological Sciences* **276:** 3971–3978.

**Bonser RHC**, **Purslow PP. 1995.** The Young modulus of feather keratin. *Journal of Experimental Biology* **1033:** 1029–1033.

**Bruderer B**, **Peter D**, **Boldt A**, **Liechti F. 2010.** Wing-beat characteristics of birds recorded with tracking radar and cine camera. *Ibis* **152:** 272–291.

**Butler LK**, **Rohwer S**, **Speidel MG. 2008.** Quantifying structural variation in contour feathers to address functional variation and life history trade-offs. *Journal of Avian Biology* **39:** 629–639.

**Cameron GJ**, **Wess TJ**, **Bonser RHC. 2003.** Young's modulus varies with differential orientation of keratin in feathers. *Journal of Structural Biology* **143:** 118–123.

**Corning WR**, **Biewener AA. 1998.** In vivo strains in pigeon flight feather shafts: implications for structural design. *The Journal of Experimental Biology* **201:** 3057–3065.

**De la Hera I**, **Hedenström A**, **Pérez-Tris J**, **Tellería JL. 2010.** Variation in the mechanical properties of flight feathers of the blackcap *Sylvia atricapilla* in relation to migration. *Journal of Avian Biology* **41:** 342–347.

**Doube M**, **Klosowski MM**, **Arganda-Carreras I**, **Cordelières FP**, **Dougherty RP**, **Jackson JS**, **Schmid B**, **Hutchinson JR**, **Shefelbine SJ. 2010.** BoneJ: free and extensible bone image analysis in ImageJ. *Bone* **47:** 1076–1079.

**Ennos A**, **Hickson J**, **Roberts A. 1995.** Functional morphology of the vanes of the flight feathers of the pigeon *Columba livia*. *The Journal of Experimental Biology* **198:** 1219–1228.

**Feo TJ**, **Field DJ**, **Prum RO. 2015.** Barb geometry of asymmetrical feathers reveals a transitional morphology in the evolution of avian flight. *Proceedings of the Royal Society B: Biological Sciences* **282:** 20142864.

**Heers AM**, **Dial KP. 2011.** From extant to extinct: locomotor ontogeny and the evolution of avian flight. *Trends in Ecology & Evolution* **27:** 296–305.

**Kato A**, **Ropert-Coudert Y**, **Grémillet D**, **Cannell B. 2006.** Locomotion and foraging strategy in foot-propelled and wing-propelled shallow-diving seabirds. *Marine Ecology Progress Series* **308:** 293–301.

**Lees J**, **Garner T**, **Cooper G**, **Nudds R. 2017.** Rachis morphology cannot accurately predict the mechanical performance of primary feathers in extant (and therefore fossil) feathered flyers. *Royal Society Open Science* **4:** 160927.

**Lees JJ**, **Dimitriadis G**, **Nudds RL. 2016.** The influence of flight style on the aerodynamic properties of avian wings as fixed lifting surfaces. *PeerJ* **4:** e2495.

**Lindhe Norberg UM. 2002.** Structure, form, and function of flight in engineering and the living world. *Journal of Morphology* **252:** 52–81.

**Macleod GD. 1980.** Mechanical properties of contour feathers. *Journal of Experimental Biology* **87:** 65–71.

**Muijres FT**, **Bowlin MS**, **Johansson LC**, **Hedenström A. 2012.** Vortex wake, downwash distribution, aerodynamic performance and wingbeat kinematics in slow-flying pied flycatchers. *Journal of the Royal Society Interface* **9:** 292–303.

**Müller W**, **Patone G. 1998.** Air transmissivity of feathers. *The Journal of Experimental Biology* **201:** 2591–2599.

**Norberg RA. 1985.** Function of vane asymmetry and shaft curvature in bird flight feathers: inferences on flight ability of *Archaeopteryx*. In: Hecht M, Ostrom J, Viohl G, Wellnhofer P, eds. *The beginnings of birds*. Eichstatt: Freunde des Jura-Museums, 303–318.

**Pap PL**, **Osváth G**, **Sándor K**, **Vincze O**, **Bărbos L**, **Marton A**, **Nudds RL**, **Vágási CI. 2015.** Interspecific variation in the structural properties of flight feathers in birds indicates adaptation to flight requirements and habitat. *Functional Ecology* **29:** 746–757.

**Pap PL**, **Vincze O**, **Wekerle B**, **Daubner T**, **Vágási CI**, **Nudds RL**, **Dyke GJ**, **Osváth G. 2017.** A phylogenetic comparative analysis reveals correlations between body feather structure and habitat. *Functional Ecology* **31:** 1241–1251.

**Pap PL**, **Vincze O**, **Vágási CI**, **Salamon Z**, **Pándi A**, **Bálint B**, **Nord A**, **Nudds RL**, **Osváth G. 2019.** Vane macrostructure of primary feathers and its adaptations to flight in birds. *Biological Journal of the Linnean Society* **126:** 256–267.

**Pennycuick CJ. 2008.** *Modelling the flying bird*. London: Academic Press.

**Pennycuick CJ. 2015.** The flight of birds and other animals. *Aerospace* **2:** 505–523.

**Purslow PP**, **Vincent JFV. 1978.** Mechanical properties of primary feathers from the pigeon. *Journal of Experimental Biology* **72:** 251–260.

**R Development Core Team. 2017.** *R: a language and environment for statistical computing*. Vienna: R Foundation for Statistical Computing. Available at: https://www.R-project.org/

**Raikow RJ. 1985.** Locomotor system. In: King A, McLelland J, eds. *Form and function in birds*. London: Academic Press, 57–147.

**Schindelin J**, **Arganda-Carreras I**, **Frise E**, **Kaynig V**, **Longair M**, **Pietzsch T**, **Preibisch S**, **Rueden C**, **Saalfeld S**, **Schmid B**, **Tinevez JY**, **White DJ**, **Hartenstein V**, **Eliceiri K**, **Tomancak P**, **Cardona A. 2012.** Fiji: an open-source platform for biological-image analysis. *Nature Methods* **9:** 676–682.

**Sullivan TN**, **Wang B**, **Espinosa HD**, **Meyers MA. 2017.** Extreme lightweight structures: avian feathers and bones. *Materials Today* **20:** 377–391.

**Tubaro PL. 2003.** A comparative study of aerodynamic function and flexural stiffness of outer tail feathers in birds. *Journal of Avian Biology* **34:** 243–250.

**Tucker V. 1993.** Gliding birds: reduction of induced drag by wing tip slots between the primary feathers. *Journal of Experimental Biology* **180:** 285–310.

**Tucker V. 1995.** Drag reduction by wing tip slots in a gliding Harris' hawk, *Parabuteo unicinctus*. *The Journal of Experimental Biology* **198:** 775–781.

**Usherwood JR. 2003.** The aerodynamics of avian take-off from direct pressure measurements in Canada geese (*Branta canadensis*). *Journal of Experimental Biology* **206:** 4051–4056.

**Usherwood JR. 2010.** The aerodynamic forces and pressure distribution of a revolving pigeon wing. *Animal Locomotion* **46:** 429–441.

**Videler JJ. 2005.** *Avian flight*. New York: Oxford University Press.

**Wang B**, **Meyers MA. 2017a.** Seagull feather shaft: correlation between structure and mechanical response. *Acta Biomaterialia* **48:** 270–288.

**Wang B**, **Meyers MA. 2017b.** Light like a feather: a fibrous natural composite with a shape changing from round to square. *Advanced Science* **4:** 1–10.

**Wang B**, **Yang W**, **McKittrick J**, **Meyers MA. 2016.** Keratin: structure, mechanical properties, occurrence in biological organisms, and efforts at bioinspiration. *Progress in Materials Science* **76:** 229–318.

**Wang X**, **Nudds RL**, **Palmer C**, **Dyke GJ. 2012.** Size scaling and stiffness of avian primary feathers: implications for the flight of Mesozoic birds. *Journal of Evolutionary Biology* **25:** 547–555.

**Weber TP**, **Kranenbarg S**, **Hedenström A**, **Waarsing JH**, **Weinans H. 2010.** Flight feather shaft structure of two warbler species with different moult schedules: a study using high-resolution X-ray imaging. *Journal of Zoology* **280:** 163–170.

**Withers PC. 1981.** The aerodynamic performance of the wing in red-shouldered hawk *Buteo linearis* and a possible aeroelastic role of wing-tip slots. *Ibis* **123:** 239–247.

**Wood SN. 2003.** Thin plate regression splines. *Journal of the Royal Statistical Society. Series B: Statistical Methodology* **65:** 95–114.

**Wood SN. 2004.** Stable and efficient multiple smoothing parameter estimation for generalized additive models. *Journal of the American Statistical Association* **99:** 673–686.

**Wood SN. 2011.** Fast stable restricted maximum likelihood and marginal likelihood estimation of semiparametric generalized linear models. *Journal of the Royal Statistical Society. Series B: Statistical Methodology* **73:** 3–36.

**Wood SN. 2017.** *Generalized additive models: an introduction with R*. Boca Raton: Chapman & Hall.

**Wood SN**, **Pya N**, **Säfken B. 2016.** Smoothing parameter and model selection for general smooth models. *Journal of the American Statistical Association* **111:** 1548–1563.

**Young WC. 1989.** *Roark's formulas for stress and strain*. New York: McGraw-Hill.

## SUPPORTING INFORMATION

Additional Supporting Information may be found in the online version of this article at the publisher's web-site:

**Table S1.** Raw data: morphological traits of the rachis.